

Generative Models From and For Sampling-Based MPC: A Bootstrapped Approach For Adaptive Contact-Rich Manipulation

Lara Bruder Müller^{1,2,*}, Brandon Hung², Xinghao Zhu², Jiuguang Wang²,
Nick Hawes¹, Preston Culbertson^{2,3,†}, Simon Le Cleac’h^{2,†}

Abstract—We present a generative predictive control (GPC) framework that amortizes sampling-based Model Predictive Control (SPC) by bootstrapping it with conditional flow-matching models trained on SPC control sequences collected in simulation. Unlike prior work relying on iterative refinement or gradient-based solvers, we show that meaningful proposal distributions can be learned directly from noisy SPC data, enabling more efficient and informed sampling during online planning. We further demonstrate, for the first time, the application of this approach to real-world contact-rich loco-manipulation with a quadruped robot. Extensive experiments in simulation and on hardware show that our method improves sample efficiency, reduces planning horizon requirements, and generalizes robustly across task variations.

I. INTRODUCTION

Reactive contact-rich (loco-)manipulation in high-dimensional state and action spaces poses significant challenges for real-time control. Sampling-based Model Predictive Control, or sampling-based predictive control (SPC), offers a principled framework to address these challenges by solving trajectory optimization problems online with a model in the loop, enabling adaptive behavior and constraint satisfaction [1]–[4]. However, the computational cost of forward simulation, combined with the challenge of effectively exploring the search space in high-dimensional, contact-rich environments, limits the applicability of real-time optimization to more complex behaviors and higher-frequency control.

To address this, a promising line of work seeks to amortize the computational burden of online optimization by shifting it to an offline phase [5]–[7]. The key idea is to collect data, either from expert demonstrations or from model-based planning, and use it to train a generative model that captures the distribution of useful actions or control sequences. At test time, this model can then be used to guide or warmstart the sampling distribution in MPC, drastically improving efficiency and solution quality by focusing sampling on high-likelihood, constraint-satisfying regions of the action space.

Recent advances in generative modeling, particularly diffusion and flow-matching models, have shown strong performance in learning expressive policies for dexterous manipulation tasks [8]–[10]. Similarly, offline model-based reinforcement learning methods [11], [12] leverage precomputed

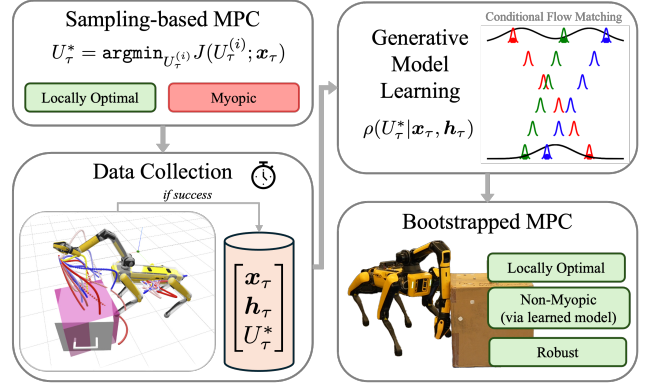


Fig. 1. *Generative predictive control (GPC) framework for bootstrapping sampling-based Model Predictive Control (SPC).* We collect open-loop control sequences from an SPC algorithm in simulation and use them to train a generative proposal distribution. At test time, this model guides and amortizes online MPC, enabling non-myopic, constraint-satisfying behavior with improved sample efficiency and robustness in contact-rich, high-dimensional settings.

data to enable fast runtime control via policy networks trained to approximate optimal solutions. Yet, these methods are often limited by the scope of their training data and struggle to generalize to out-of-distribution (OOD) states or tasks. In response to these limitations, several recent works demonstrate that bootstrapping online planners with offline-trained generative models leads to faster convergence, better exploration, and more robust performance in complex environments [7], [13]–[15]. In this paper, we adopt this amortized optimization perspective, focusing on how offline data collection and generative modeling can be used to accelerate and guide online sampling-based MPC in contact-rich, high-dimensional settings while maintaining the flexibility and adaptability of online optimization.

Contributions: We propose a *generative predictive control (GPC) framework that bootstraps SPC with conditional flow-matching models trained on SPC control sequences collected in simulation.* To the best of our knowledge, we are the first to show that meaningful *proposal distributions can be learned directly from noisy SPC data without requiring expert refinement or numerical solvers.* We are also the first to demonstrate this approach on *real hardware in a contact-rich loco-manipulation task*, and show that it improves sample efficiency and *generalizes robustly to task variations in both simulation and real world.*

¹Oxford Robotics Institute, University of Oxford, UK.

²Robotics and AI Institute (RAI), Boston, USA.

³Cornell University, Ithaca, NY, USA.

*This work was conducted while Lara Bruder Müller was an intern at the Robotics and AI Institute.

†Preston Culbertson and Simon Le Cleac’h advised this work equally.

II. RELATED WORK

SPC for Contact-Rich Manipulation: SPC has been widely adopted for its robustness to nonlinearity, discontinuities, and nonconvexities, particularly in contact-rich robotic tasks [1]–[3], [16]–[19]. These methods typically optimize a trajectory distribution by iteratively sampling candidate controls and selecting elites based on forward-simulated costs. However, their performance is often limited by the computational cost of forward dynamics, especially when simulating contact interactions or systems with many degrees of freedom (DOF). While prior work has sought to speed up forward simulation, e.g., via quasi-static approximations [20] or learned dynamics models [21], these approaches often trade off fidelity or depend on highly accurate model learning. In contrast, we do not aim to replace the dynamics model but rather to amortize the trajectory optimization itself. We do this by learning generative models over control distributions derived from open-loop control sequences that either led to task success or incurred low cost in offline sampling-based MPC, enabling faster and more informed sampling at test time.

Amortizing Online Optimization via Offline Learning: Recent work leverages offline data to reduce the computational burden of control algorithms at runtime. Learning from expert demonstrations or planner rollouts, via behavior cloning [8]–[10] or model-based RL [11], [12], has become a common approach. When sourced from high-quality planners, such as sampling-based MPC, this data enables training generative models that can guide or initialize online control. Several works have explored learning from planner-generated trajectories to approximate optimal or near-optimal solutions and accelerate planning [6], [22]–[24]. This idea underpins Approximate MPC (AMPC), where learned models bootstrap or replace expensive solvers. Early efforts used regression or Gaussian Mixture Models to represent multi-modal action distributions [25], [26], while recent work adopts diffusion and flow-matching models for their expressiveness [7], [27], [28]. For instance, [29] use diffusion models to approximate near-globally optimal MPC solutions from locally optimal trajectories generated by a numerical solver [30]. At runtime, a sample-score-rank strategy is applied to select the best candidate sampled from the learned distribution. While conceptually similar to our approach, their results are limited to simple environments due to the slow inference speed of the diffusion model. Our work is most closely related to Kurtz et al. [14], who also bootstrap SPC using generative models trained on SPC control sequences. Their method uses *online* data, performing iterative training that alternates between data collection and model updates, using controls sampled from each partially trained model. While this strategy aims to improve the quality of the training data, we find empirically that it can, in fact, degrade performance by collapsing the multi-modal structure of the control sequence distribution, crucial for effective sampling. In contrast, our method trains a generative model over *offline* data (noisy SPC rollouts) and achieves strong performance, showing that bootstrapped SPC

does not require iterative refinement. To our knowledge, [14] and our work are the first to learn from SPC data, rather than from trajectories generated by gradient-based solvers.

Learning Sampling Distributions for Online MPC: Another line of work aims to improve SPC by learning structured priors over control sequences in latent action spaces using generative models [31], [32]. These methods typically rely on expert demonstrations, which lack exploratory diversity, and require complex bi-level training to learn both latent spaces and their distributions. In contrast, we focus on directly leveraging the diverse data that can be produced by sampling-based MPC in an offline data collection setting. Freed from real-time constraints, we can expand the search space during planning, yielding richer control sequences that support efficient sampling through simpler generative models at test time.

III. BACKGROUND

A. Problem Formulation

In this paper we consider optimal control problems in continuous action spaces. Given an initial state $\mathbf{x}_0 = \mathbf{x}_{init}$, the objective is to determine a sequence of open-loop control actions $U_\tau = [\mathbf{u}_\tau, \mathbf{u}_{\tau+1}, \dots, \mathbf{u}_{\tau+T}]$ that minimizes a given cost function over a finite time horizon T :

$$\min_{\mathbf{u}_0, \mathbf{u}_1, \dots, \mathbf{u}_T} \phi(\mathbf{x}_{T+1}) + \sum_{\tau=0}^T \ell(\mathbf{x}_\tau, \mathbf{u}_\tau) \quad (1a)$$

$$\text{s.t. } \mathbf{x}_{\tau+1} = f(\mathbf{x}_\tau, \mathbf{u}_\tau), \quad \tau = 0, \dots, T \quad (1b)$$

$$\mathbf{x}_0 = \mathbf{x}_{init}, \quad (1c)$$

where $\mathbf{x}_\tau \in \mathbb{R}^n$ and $\mathbf{u}_\tau \in \mathbb{R}^m$ are the state vector and the control input at time step τ , respectively. The functions $\ell : \mathbb{R}^n \times \mathbb{R}^m \rightarrow \mathbb{R}$ and $\phi : \mathbb{R}^n \rightarrow \mathbb{R}$ represent the stage and terminal cost, respectively. We do not assume to know the closed-form expression for the system dynamics $f : \mathbb{R}^n \times \mathbb{R}^m \rightarrow \mathbb{R}^n$, but instead assume access to a simulator (e.g. MuJoCo [33]) or a learned model. For a more compact notation, we define a cost function $J : \mathbb{R}^{m \times T} \times \mathbb{R}^n \rightarrow \mathbb{R}$ that encapsulates both, costs and system dynamics, allowing us to write the problem as

$$\min_U J(U; \mathbf{x}_{init}). \quad (2)$$

Rather than deriving a single, globally optimal policy, MPC re-optimizes a local policy at each time step by simulating the system dynamics over a shorter receding horizon $H < T$.

B. Sampling-based MPC (SPC)

Contact-rich robot control tasks pose significant challenges due to the non-convexity of cost functions and the nonlinear, often discontinuous nature of system dynamics. Sampling-based MPC addresses these issues by optimizing over a parameterized distribution $\pi_\phi(U)$ rather than directly computing the optimal control sequence.

We consider a generic SPC procedure in which, at each control step τ , the controller samples N control sequences $\{U^{(i)}\}_{i=1}^N$ from the current distribution π_ϕ , simulates their

outcomes from the current state estimate $\hat{\mathbf{x}}_\tau$, and evaluates them using the cost function $J(U^{(i)}; \hat{\mathbf{x}}_\tau)$. Based on these evaluations, the distribution parameters ϕ are updated according to the specific SPC algorithm used. The executed control \mathbf{u}_τ is typically the first element of \bar{U}_τ , or alternatively, it can be derived via spline interpolation across the optimized sequence. While other works explore non-Gaussian proposal distributions [31], we focus on diagonal Gaussian distributions of the form $\pi_\phi(U) = \mathcal{N}(\bar{U}, \Sigma)$, as used in the Cross-Entropy Method (CEM) [34] and other SPC algorithms [2], [16]. Here, $\phi = (\bar{U}, \Sigma)$, and $\Sigma = \text{diag}(\mathbf{s})$, with \mathbf{s} denoting a vector of variances across dimensions.

C. Generative Modeling: Flow-Matching

While the above focuses on shaping a sampling distribution for SPC, generative modeling focuses on a different problem: produce a sample x from a target distribution $p(x)$, which is typically unknown in closed form, but can be approximated by a dataset of samples \mathcal{D} . Among recent approaches to generative modeling, two closely related approaches have gained significant traction due to their ability to capture complex, multi-modal distributions: flow matching [35] and diffusion models [36]. The underlying concept is to learn a distribution over trajectories or transformations that maps a simple prior distribution to complex target data. In this work, we focus on flow-matching models and their conditional variant [37], as they offer superior inference speed compared to diffusion models. Flow matching aims to learn a time-dependent vector field $v_\theta(\mathbf{x}, t)$ that transports samples from an easy-to-sample prior distribution $p_0(\mathbf{x})$ (e.g., a standard Gaussian) to a target data distribution $p_1(\mathbf{x})$. The flow network v_θ is trained on

$$\min_{\theta} \mathbb{E}_{\substack{\mathbf{x}_0 \sim p_0, \\ \mathbf{x}_1 \sim p_1, \\ t \sim \mathcal{U}(0,1)}}} \left[\|v_\theta(t\mathbf{x}_1 + (1-t)\mathbf{x}_0, t) - (\mathbf{x}_1 - \mathbf{x}_0)\|^2 \right] \quad (1)$$

This loss encourages the vector field to push samples along straight-line paths from \mathbf{x}_0 to \mathbf{x}_1 . At inference time, new samples are generated by drawing $\mathbf{x}_0 \sim p_0(\mathbf{x})$ and solving the ODE $\dot{\mathbf{x}} = v_\theta(\mathbf{x}, t)$ from $t = 0$ to $t = 1$, typically approximated with an Euler scheme $\mathbf{x}_{t+\delta t} = \mathbf{x}_t + v_\theta(\mathbf{x}_t, t)\delta t$.

IV. BOOTSTRAPPING SAMPLING-BASED MPC WITH GENERATIVE FLOW-MATCHING MODELS

In this section, we introduce our approach for bootstrapping SPC with generative models trained on open-loop control sequences collected from SPC itself. The core idea is to learn a generative model that approximates the distribution of successful control sequences conditioned on the current state and history. At test time, this model serves as a proposal distribution to guide and warm-start the sampling process in online SPC, improving sample efficiency and robustness.

A. Data collection

The offline data collection phase is central to our approach, as it should provide control sequences, that are likely to lead to task success, conditioned on the current state and history of states. Since we aim to bootstrap SPC at test time,

we generate this dataset directly from an SPC algorithm, specifically CEM as it is widely used and easy to tune for different tasks, without the runtime constraints of online control. This allows for longer horizons and larger sample sizes to collect high-quality, non-myopic control sequences.

Given a task and associated cost function, we run the SPC algorithm across multiple episodes, each with random state initializations and capped at a maximum number of MPC iterations. During each episode, we record tuples of the form $(\mathbf{x}_\tau, \mathbf{h}_\tau, U_\tau^*)$, where \mathbf{x}_τ is the current state, \mathbf{h}_τ encodes a fixed-window history of states, and U_τ^* denotes the mean control sequence of the CEM distribution at time τ . An experiment is considered successful if the task is completed within the allowed time steps. We define $\mathcal{I}_{\text{success}}$ as the index set of all successful experiment episodes, and construct our training dataset as

$$\mathcal{D} = \bigcup_{i \in \mathcal{I}_{\text{success}}} \{(\mathbf{x}_\tau^{(i)}, \mathbf{h}_\tau^{(i)}, U_\tau^{*(i)})\}_{\tau=0}^{T_i},$$

where T_i is the final time step of episode i . This ensures that only control sequences from successful rollouts are used to train the generative model.

To reduce the complexity of the generative model and improve runtime efficiency, as well as smoothness, each control sequence U_τ is represented using $K < H$ control points over a planning horizon of H time steps, i.e. $U = [\mathbf{u}_0, \mathbf{u}_1, \dots, \mathbf{u}_K]$. These control points may correspond to spline knots or waypoints for linear interpolation. We also employ *i*) a progress-based heuristic to reset the variances during CEM in order to avoid early mode collapse, and *ii*) action-level annealing [18] that increases exploration, i.e., variances, for control points further into the horizon.

B. Learning Control Sequence Proposal Distributions

Once we have collected a dataset of open-loop trajectories for a given task, we can train a flow-matching generative model to learn a time-varying state-conditional vector field $v_\theta(U, \mathbf{x}_\tau, \mathbf{h}_\tau, t)$ that pushes samples from $U_t \sim \mathcal{N}(0, I)$ at flow step $t = 0$ to the target distribution $U_{t=1} \sim p_\theta(U | \mathbf{x}_\tau, \mathbf{h}_\tau)$ at $t = 1$, i.e. the distribution of control sequences that are likely to lead to successful task completion given the current state \mathbf{x}_τ and state history \mathbf{h}_τ . For simplicity, we summarize samples from the generative model as samples from the distribution $p_\theta(U | \mathbf{x}_\tau, \mathbf{h}_\tau)$. We refer to our method as generative predictive control (GPC), which leverages a learned distribution over control sequences conditioned on task context. This distribution can be used in two distinct ways: *i*) as a sampling distribution in a random shooting approach, where we sample a batch of control sequences from p_θ and select the best candidate based on the rollouts and their respective costs, or *ii*) in conjunction with an SPC algorithm, where samples from $p_\theta(U | \mathbf{x}_\tau)$ are used to update the sampling distribution of the SPC algorithm, e.g., $\pi_\phi(U)$ in the CEM. In the following, we call the first approach *GPC-Shoot* and the second approach *GPC-CEM*.

Algorithm 1: GPC-CEM

Input: Current state \mathbf{x}_τ , history \mathbf{h}_τ
Sampling distribution $\pi_\phi(U) = \mathcal{N}(\bar{U}, \Sigma)$
Flow model $p_\theta(U | \mathbf{x}_\tau, \mathbf{h}_\tau)$
Number of rollouts $N = N_{\text{CEM}} + N_{\text{Flow}}$
Number of elites N_{elite}
State estimator $\hat{\mathbf{x}}(\tau)$

while planning do

- $\mathbf{x}_0 \leftarrow \hat{\mathbf{x}}(\tau)$ // Get current state estimate
- Sample N_{CEM} trajectories from CEM:
 $\{U^{(i)}\}_{i=1}^{N_{\text{CEM}}} \sim \pi_\phi(U)$
- Sample N_{Flow} trajectories from flow model:
 $\{U^{(j)}\}_{j=1}^{N_{\text{Flow}}} \sim p_\theta(U | \mathbf{x}_\tau, \mathbf{h}_\tau)$
- Compute $\{J^{(k)} \leftarrow J(U^{(k)}; \mathbf{x}_0)\}_{k=1}^N$ // parallel rollouts
- Select top N_{elite} elite trajectories with lowest cost:
 $\{U^{(k)}\}_{k=1}^{N_{\text{elite}}} \leftarrow \text{elite set}$
- Update $\pi_\phi(U)$ using elite statistics:
 $U^* \leftarrow U^{(k^*)}, \quad k^* = \arg \min_k J^{(k)}$
 $\bar{U} \leftarrow \text{shift}(U^*, \tau)$ // shift mean forward
 $\Sigma \leftarrow \text{diag}(\text{Var}(\{U^{(k)}\}))$
- Execute control $\mathbf{u}_\tau \leftarrow \text{get_action}(U^*, \tau)$
- Update state history $\mathbf{h}_{\tau+1} \leftarrow \text{roll}(\mathbf{h}_\tau, \mathbf{x}_\tau)$

C. GPC-CEM: Bootstrapping SPC with Flow-Matching

Trained on a finite set of open-loop control sequences, the generative proposal distribution $p_\theta(U | \mathbf{x}_\tau, \mathbf{h}_\tau)$ inherits the generalization limitations of behavior cloning and model-based RL. This sensitivity to distributional shifts, something we also observe in our experiments with GPC-Shoot, manifests as degraded sample quality from the proposal distribution in a small subset of states, particularly when the object enters regions underrepresented in the training data. In contrast, SPC adapts its sampling distribution online and is more robust in such situations, though it remains myopic and computationally expensive. To balance these trade-offs, we bootstrap SPC with a flow-matching generative model that approximates the dataset’s control distribution while preserving the adaptability of online sampling during execution. We summarize our approach in Algorithm 1. At each control step, the algorithm begins by estimating the current state and shifting the current mean of the CEM sampling distribution forward in time. The key idea in GPC-CEM is to augment Gaussian CEM sampling with proposals from the generative model p_θ trained offline on control sequences that led to task success. Proposals yielding low-cost rollouts are used to update the CEM distribution $\pi_\phi(U)$, with the mean set to the time-shifted best candidate, and the variance is computed from the elite set, thereby adapting it toward higher-quality actions. Unlike standard CEM, the executed control is not derived from the elite mean, which assumes unimodality, but instead taken from the best-performing candidate, allowing GPC-CEM to better exploit multimodal proposals from the generative model. This hybrid approach efficiently guides exploration while maintaining the adaptability of online optimization.

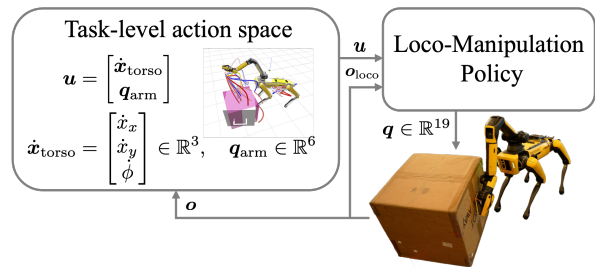


Fig. 2. The mapping from the high-level action space to the low-level spot loco-manipulation control space. The locomotion policy is pre-trained to follow the high-level commands while maintaining balance and stability. It is fixed throughout the full task planning and execution.

D. Application to Loco-Manipulation

We apply our bootstrapped SPC framework to non-prehensile object pushing with a Spot quadruped robot with an arm to demonstrate versatile loco-manipulation skills. With 19 degrees of freedom (DoF), planning for this robot is computationally expensive, especially in SPC, where higher dimensionality typically demands for larger sample sizes. To simplify the task, based on the work of [38], we disentangle the low-level locomotion control from the high-level task-level action space, as illustrated in Fig. 2. The high-level action space includes 9 DoF (3 for the torso, 6 for the arm)¹ and is mapped to low-level commands by a pre-trained locomotion policy that ensures balance and stability while tracking high-level inputs. The low-level locomotion policy is fixed throughout task planning and execution. Besides the lower-dimensional action space, a core advantage of this approach is that this hierarchical control structure naturally provides more robustness to the low-level control, removing the need to introduce guidance terms that explicitly enforce smoothness and temporal consistency of the control sequences into the flow-matching process.

V. EXPERIMENTAL RESULTS

We evaluate our proposed GPC framework across simulated and real-world continuous control tasks involving contact-rich, non-prehensile manipulation. Specifically, we benchmark performance on *i*) the well-known Push-T task with a 2-DoF circular robot, and *ii*) the loco-manipulation task introduced above. To guide our evaluation, we aim to answer the following key questions: *i*) How well does the learned generative model approximate the action proposal distribution captured by open-loop sampling-based MPC? *ii*) Does bootstrapping online MPC with a learned proposal distribution improve *task performance* and *generalization to task variations* under constrained computational budgets?

We use conditional flow matching to train a generative model over SPC control sequences with a simple Multi-Layer Perceptron (MLP) as the underlying architecture. We consider both direct sampling from the learned model (*GPC-Shoot*) and the bootstrapped version that combines it with

¹We exclude the gripper DoF from the high-level action space for non-prehensile manipulation. Yet, this and additional DoF (e.g., torso height, pitch, roll) could be included without retraining the low-level policy.

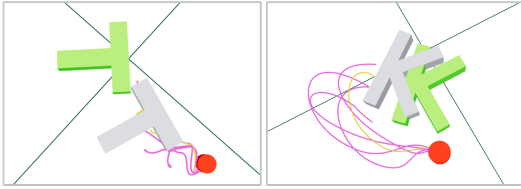


Fig. 3. **Push-T Task overview.** *Left:* Original Push-T task [9], where a circular robot is required to push a T-shaped block into a target pose, shown in green. *Right:* Modified task with a K- instead of T-block at the bottom.

CEM-based online planning (*GPC-CEM*). We compare our approach against standard CEM, as well as model predictive path integral control (MPPI) [16] and DialMPC [18], a more recent SPC approach building on MPPI. We only compare against DialMPC on the Push-T task, as its inner optimization loop doubles simulation time, making it unsuitable for real-time loco-manipulation. All methods are implemented in Python using `judo` [39], which provides a unified interface for defining custom tasks and controllers. For each task, we evaluate all methods with the same number of rollouts per iteration, control frequency, and respective cost function. In addition, we report results for the GPC-methods across three different model seeds to account for the stochasticity in the training process. We set the CEM-sample ratio in GPC-CEM, i.e. N_{CEM}/N , to 0.5 for both tasks.

A. Push-T Task

This task requires a 2-DoF circular robot to push a T-shaped block into a specified goal pose. Due to its sparse rewards and multi-modality, it serves as a popular benchmark for evaluating generative control policies. We also evaluate the adaptability of GPC to novel, unseen task variations without retraining by running it on a variant where the T-shaped block is replaced with a K-shaped block (Push-K), introducing different object dynamics. In this setting, we reuse the generative model trained on Push-T to bootstrap SPC for Push-K, showcasing GPC’s robustness and ability to generalize across task variations. Table I summarizes the simulation results. We report success rates with Wilson 95% confidence intervals and average completion times (for successful runs) with respective standard deviations based on 1000 trials per method. Success is defined as achieving at least 0.9 coverage of the target pose within 2500 time steps (0.01 s each). For GPC-CEM, we additionally report the average CEM sample ratio and standard deviation, indicating how often samples were selected from the CEM distribution over the learned proposal distribution.

Both CEM and DIAL-MPC [18] achieve high success rates ($\geq 85\%$), demonstrating the strength of sampling-based methods. While DIAL-MPC includes an inner optimization loop, its gains over CEM are marginal and come at higher computational cost; thus, we use CEM for data collection. MPPI performs moderately (62% success), though better tuning may close this gap. GPC-Shoot performance improves with more denoising steps (indicated in parentheses): 99% success with 10 steps vs. 71% with 2. Similarly, GPC-CEM with 10 steps not only achieves 99.8% success but

also reduces completion time by nearly 50% compared to 2 steps. Notably, GPC-CEM remains robust under reduced horizons (1s vs. 3s), maintaining 96% success versus 78% for CEM. This suggests that our method enables non-myopic planning under tighter computational constraints. In the Push-K generalization task, GPC-CEM again outperforms all baselines, achieving 96% success compared to 55% for CEM, indicating strong transferability of the learned proposal distribution. This is a notable insight, as CEM performance drops significantly without any changes to the cost function, highlighting that the learned distribution captures meaningful structural priors useful across tasks.

Comparison to Iterative Training Procedure [14]: We acknowledge the conceptual similarity between our approach and that of Kurtz et al. [14], who also combine generative modeling with SPC. However, their method adopts an iterative training procedure that alternates between data collection and model updates, similar to expert iteration in reinforcement learning [40]. This setup is motivated by the assumption that SPC data is too noisy to directly train a generative model; hence, each data collection iteration bootstraps SPC with a partially trained flow-matching model to improve the subsequent training distribution. In our experiments on the Push-T task, however, this iterative procedure did not improve performance (see Fig. 4). In fact, success rates declined over training iterations. We attribute this to a reduction in multi-modality of the learned proposal distribution, which is critical for sampling-based MPC in tasks with multiple distinct solution modes. This interpretation is supported by the decreasing CEM sample ratio over training iterations, suggesting that the learned proposal increasingly matches the uni-modal CEM distribution, making the two distributions interchangeable rather than complementary. In contrast, our method trains a generative model directly on open-loop control sequences from SPC, without requiring iterative retraining. Despite the noisy data, our model achieves up to 99.2% success (GPC-Shoot with 10 denoising steps), and already reaches 96% when bootstrapped with CEM after a single training round.

B. Spot Loco-Manipulation

In this task, Spot must push a chair into a goal pose located behind a C-shaped obstacle (Fig. 5). The robot and chair are always initialized randomly on the opposite side of the obstacle, creating a local minimum that requires navigating around it to succeed. The task is further complicated by the high-dimensional action space and contact dynamics. Solving this with SPC demands long horizons and large sample sizes, both of which increase computational cost. A trial is considered successful if the chair’s position error is below 0.15 m and its yaw is within 50 degrees of the target.

Simulation: We first evaluate the task in simulation to enable larger-scale testing. Results are summarized in Table II. Each baseline is run for 100 trials, and GPC methods are evaluated with 3 model seeds (100 trials each). We omit DIAL-MPC due to its inner-loop optimization being too slow for real-time use in this task. As in Push-T, we

Control frequency: 10 Hz Time step (Δt): 0.01 s Rollouts: 32			
	Success rate (\uparrow)	Number of steps (success only, (\downarrow))	CEM sample ratio
<i>Base Task: Push-T</i>			
CEM Baseline	0.85 (0.83, 0.88)	1037.57 \pm 526.40	–
MPPI Baseline	0.62 (0.59, 0.65)	1634.15 \pm 492.42	–
Dial-MPC [18]	0.86 (0.83, 0.88)	1197.07 \pm 461.16	–
GPC-Shoot (2)	0.718 (0.702, 0.734)	1277.51 \pm 572.80	–
GPC-Shoot (10)	0.992 (0.988, 0.995)	608.58 \pm 291.48	–
GPC-CEM (2)	0.980 (0.980, 0.985)	932.40 \pm 449.95	0.33 \pm 0.11
GPC-CEM (10)	0.998 (0.996, 0.999)	591.11 \pm 267.20	0.33 \pm 0.10
<i>Horizon Ablation: using 1 secs. instead of 3 secs. at inference time</i>			
CEM Baseline	0.78 (0.76, 0.81)	1093.50 \pm 523.09	–
MPPI Baseline	0.68 (0.65, 0.71)	1365.65 \pm 463.48	–
Dial-MPC [18]	0.84 (0.81, 0.86)	945.76 \pm 403.05	–
GPC-Shoot (10)	0.84 (0.83, 0.85)	978.96 \pm 543.72	–
GPC-CEM (10)	0.96 (0.95, 0.97)	890.42 \pm 466.94	0.42 \pm 0.08
<i>Task Variation: Push-K</i>			
CEM Baseline	0.55 (0.52, 0.58)	1143.21 \pm 565.90	–
MPPI Baseline	0.34 (0.31, 0.36)	1707.92 \pm 501.53	–
Dial-MPC [18]	0.56 (0.52, 0.59)	1333.13 \pm 484.97	–
GPC-Shoot (10)	0.89 (0.88, 0.90)	1015.15 \pm 527.04	–
GPC-CEM (10)	0.96 (0.95, 0.96)	887.77 \pm 482.02	0.41 \pm 0.10

TABLE I

SIMULATION RESULTS FOR THE PUSH-T TASK, INCLUDING A HORIZON ABLATION AND A TASK VARIATION WITH A K- INSTEAD OF A T-BLOCK.

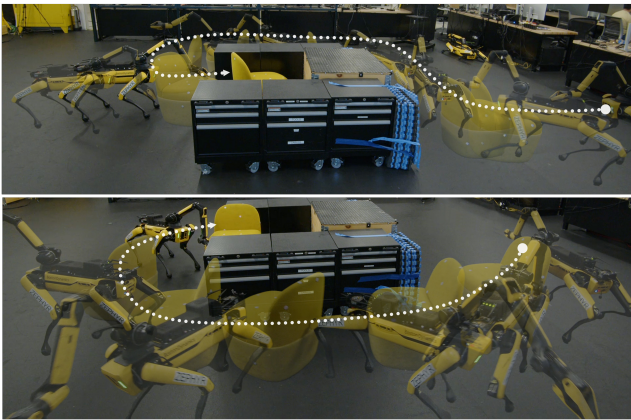


Fig. 5. **Spot Loco-Manipulation Experiment:** Qualitative examples of two successful Spot loco-manipulation task runs in the real world with GPC-CEM. Both images show an overlay of several snapshots of the trajectories of the robot and the chair.

report success rate, average completion steps (for successful runs), and CEM sample ratio. GPC-CEM outperforms all baselines, achieving up to 83% success with fewer executed steps. In contrast, CEM alone reaches only 33%, often failing due to limited horizon and sample budget. MPPI performs slightly better but remains unreliable under real-time constraints. GPC-CEM remains robust under reduced planning horizons (3 vs. 4 seconds), maintaining 60% success, while baseline performance degrades. This reinforces that learned proposals can enhance planning in resource-limited settings.

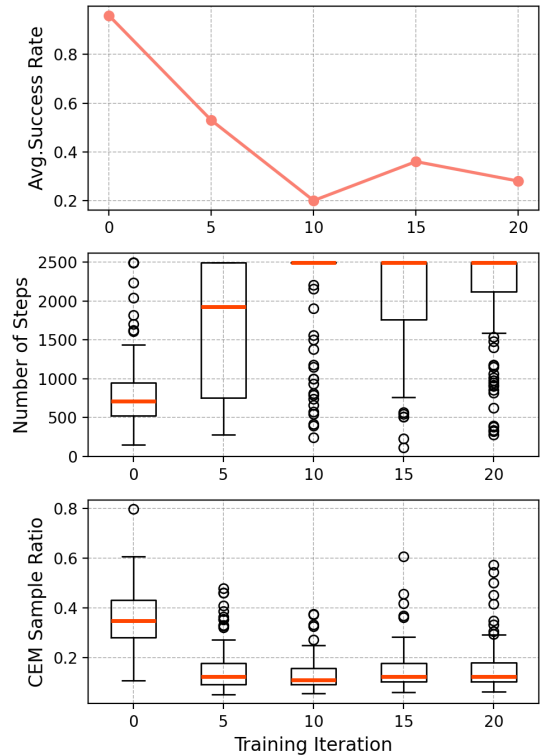


Fig. 4. Evaluation of intermediate models from the iterative training procedure from [14] on the Push-T task. Results are shown for 100 experiments per iteration.

Interestingly, fewer denoising steps (2 vs. 10) yield better performance in this task for both GPC-Shoot and GPC-CEM. We attribute this to reduced sample diversity at higher step counts, which impairs exploration in tasks with deceptive local minima. We also observe higher CEM sample ratios in this task compared to Push-T, indicating that the learned model alone (GPC-Shoot) is less accurate. Instead, it is most effective when used to augment CEM, highlighting the value of integrating learned proposals into online optimization rather than relying on them directly. Finally, we evaluate a task variant with an added obstacle avoidance cost to prevent collisions with the C-shaped obstacle. While omitted from the base task to avoid biasing the MPC methods, this constraint is essential for real-world deployment. In this setting, GPC-CEM still leads with a 56% success rate, outperforming MPPI (30%) and CEM (27%).

Real-World: We evaluate GPC-CEM and CEM on hardware including the obstacle avoidance cost in both cases. We rely on a Motion Capture system to track the current object state. GPC-CEM is run with 2 denoising steps for 20 trials, while CEM is limited to 10 trials due to frequent damaging failures to the robot, such as repeated collisions with the obstacle as it fails to navigate around. **GPC-CEM** achieves a **60% success rate (12/20)**, while **CEM** succeeds in only **10% of trials (1/10)**. Qualitative examples for GPC-CEM are shown in Fig. 5; all other runs are included in the supplementary video². CEM failures consistently result

²<https://youtu.be/1KCGjjddv1E>

<i>Control frequency: 5 Hz Time step (Δt): 0.02 s Rollouts: 32</i>			
	Succ. rate (\uparrow)	Number of steps (success only, (\downarrow))	CEM sample ratio
<i>Base Task: Spot Loco-Manipulation</i>			
CEM Baseline	0.33 (0.28, 0.39)	1452.1 \pm 448.2	–
MPPI Baseline	0.57 (0.51, 0.62)	1096.3 \pm 360.6	–
GPC-Shoot (2)	0.18 (0.14, 0.23)	1544.6 \pm 495.2	–
GPC-Shoot (10)	0.22 (0.18, 0.27)	1454.2 \pm 511.5	–
GPC-CEM (2)	0.83 (0.78, 0.87)	1125.9 \pm 430.6	0.69 \pm 0.10
GPC-CEM (10)	0.79 (0.74, 0.83)	1073.9 \pm 367.4	0.66 \pm 0.11
<i>Horizon Ablation: using 3 secs. instead of 4 secs. at inference time</i>			
CEM Baseline	0.26 (0.21, 0.31)	1494.6 \pm 491.9	–
MPPI Baseline	0.29 (0.24, 0.34)	1177.3 \pm 465.3	–
GPC-Shoot (2)	0.22 (0.18, 0.27)	1489.3 \pm 498.7	–
GPC-CEM (2)	0.60 (0.54, 0.65)	1135.3 \pm 487.9	0.71 \pm 0.08
<i>Task Variation: Spot Loco-Manipulation with Obstacle Avoidance</i>			
CEM Baseline	0.27 (0.22, 0.32)	1692.3 \pm 439.7	–
MPPI Baseline	0.30 (0.25, 0.35)	1634.2 \pm 473.9	–
GPC-Shoot (2)	0.03 (0.02, 0.06)	1764.5 \pm 353.2	–
GPC-CEM (2)	0.56 (0.50, 0.62)	1421.1 \pm 481.8	0.74 \pm 0.08

TABLE II

SIMULATION RESULTS FOR THE SPOT LOCO-MANIPULATION TASK, INCLUDING HORIZON ABLATION AND TASK VARIATION WITH ADDITIONAL OBSTACLE AVOIDANCE COST AT RUNTIME.

from getting stuck in the local minimum caused by the C-shaped obstacle, as it lacks the guidance from the generative model to sample motions that navigate around it. GPC-CEM only encounters this failure in 4 of 20 trials. The remaining failures stem from two causes: (1) pushing the chair beyond the workspace due to the lack of workspace constraints in the cost, and (2) discrepancies between simulated and real chair behavior, especially when assumptions about friction and contact are violated, such as when the chair’s wheels are unable to roll. We intentionally excluded workspace limits to evaluate the methods with minimal guidance.

Computation Time: Finally, we analyze the computation time per MPC iteration, finding that the dominant bottleneck remains policy rollout, which accounts for over 90% of the total compute time, limiting the overall control frequency to 5 Hz. This overhead is primarily due to collision handling and contact dynamics in the physics engine.

VI. LIMITATIONS

One limitation of our framework is that it does not explicitly address sim-to-real transfer, leaving it vulnerable to discrepancies between simulated and real-world dynamics. However, since our method relies on offline data collection, it can be trained on domain-randomized data, which we expect to improve robustness to variations in dynamics, actuator behavior, and sensor noise, as suggested by prior work [14]. In this work, all experiments consider fixed goals. We plan to extend our work to variable goals by transforming our data into goal-centric representations. The current system also does not use GPU acceleration for forward simulation or inference with the flow-matching model, but this could be

addressed in future work to enable faster online planning and data collection, especially with larger sample sizes. Finally, the proposed approach is limited to state-based policies but can be extended to vision-based policies by learning from observations collected while executing the state-based policy in the real world or simulation. Future work should explore how to integrate vision-based action proposal distributions with fast vision-based dynamics models for online predictive control, similar to [13].

VII. CONCLUSION

We presented GPC-CEM, a generative predictive control (GPC) framework that bootstraps sampling-based MPC (SPC) with conditional flow-matching trained on open-loop SPC control sequences. Our approach demonstrates that meaningful proposal distributions can be learned directly from noisy SPC data, without expert supervision or iterative refinement. We evaluated our method in two challenging settings; a simulated pushing benchmark and a real-world quadruped loco-manipulation task; and showed that it significantly improves sample efficiency and robustness. GPC-CEM achieves high success rates, remains effective under reduced planning horizons, and generalizes to task variations which introduce out-of-distribution conditions. These results highlight the effectiveness of integrating learned generative models into online optimization loops for efficient and adaptable real-time robot control.

REFERENCES

- [1] A. H. Li, P. Culbertson, V. Kurtz, and A. D. Ames, “Drop: Dexterous reorientation via online planning,” *arXiv preprint arXiv:2409.14562*, 2024.
- [2] T. Howell, N. Gileadi, S. Tunyasuvunakool, K. Zakka, T. Erez, and Y. Tassa, “Predictive sampling: Real-time behaviour synthesis with mujoco,” *arXiv preprint arXiv:2212.00541*, 2022.
- [3] J. Jankowski, L. Bruder Müller, N. Hawes, and S. Calinon, “Vp-sto: Via-point-based stochastic trajectory optimization for reactive robot behavior,” in *2023 IEEE International Conference on Robotics and Automation (ICRA)*. IEEE, 2023, pp. 10 125–10 131.
- [4] M. Bhardwaj, B. Sundaralingam, A. Mousavian, N. D. Ratliff, D. Fox, F. Ramos, and B. Boots, “Storm: An integrated framework for fast joint-space model-predictive control for reactive manipulation,” in *Conference on Robot Learning*. PMLR, 2022, pp. 750–759.
- [5] B. Ichter, J. Harrison, and M. Pavone, “Learning sampling distributions for robot motion planning,” in *2018 IEEE International Conference on Robotics and Automation (ICRA)*. IEEE, 2018, pp. 7087–7094.
- [6] A. Fishman, A. Murali, C. Eppner, B. Peele, B. Boots, and D. Fox, “Motion policy networks,” in *conference on Robot Learning*. PMLR, 2023, pp. 967–977.
- [7] G. Zhou, S. Swaminathan, R. V. Raju, J. S. Guntupalli, W. Lehrach, J. Ortiz, A. Dedieu, M. Lázaro-Gredilla, and K. Murphy, “Diffusion model predictive control,” *arXiv preprint arXiv:2410.05364*, 2024.
- [8] K. Black, N. Brown, D. Driess, A. Esmail, M. Equi, C. Finn, N. Fusai, L. Groom, K. Hausman, B. Ichter *et al.*, “ π 0: A vision-language-action flow model for general robot control, 2024,” *arXiv preprint arXiv:2410.24164*, 2024.
- [9] C. Chi, Z. Xu, S. Feng, E. Cousineau, Y. Du, B. Burchfiel, R. Tedrake, and S. Song, “Diffusion policy: Visuomotor policy learning via action diffusion,” *The International Journal of Robotics Research*, p. 02783649241273668, 2023.
- [10] T. Z. Zhao, V. Kumar, S. Levine, and C. Finn, “Learning fine-grained bimanual manipulation with low-cost hardware,” *arXiv preprint arXiv:2304.13705*, 2023.
- [11] N. Hansen, H. Su, and X. Wang, “Td-mpc2: Scalable, robust world models for continuous control,” *arXiv preprint arXiv:2310.16828*, 2023.

- [12] I. Dadiotis, M. Mittal, N. Tsagarakis, and M. Hutter, “Dynamic object goal pushing with mobile manipulators through model-free constrained reinforcement learning,” *arXiv preprint arXiv:2502.01546*, 2025.
- [13] H. Qi, H. Yin, Y. Du, and H. Yang, “Strengthening generative robot policies through predictive world modeling,” *arXiv preprint arXiv:2502.00622*, 2025.
- [14] V. Kurtz and J. W. Burdick, “Generative predictive control: Flow matching policies for dynamic and difficult-to-demonstrate tasks,” *arXiv preprint arXiv:2502.13406*, 2025.
- [15] Y. Wang, H. Guo, S. Wang, L. Qian, and X. Lan, “Bootstrapped model predictive control,” *arXiv preprint arXiv:2503.18871*, 2025.
- [16] G. Williams, A. Aldrich, and E. A. Theodorou, “Model predictive path integral control: From theory to parallel computation,” *Journal of Guidance, Control, and Dynamics*, vol. 40, no. 2, pp. 344–357, 2017.
- [17] M. Kobilarov, “Cross-entropy motion planning,” *The International Journal of Robotics Research*, vol. 31, no. 7, pp. 855–871, 2012.
- [18] H. Xue, C. Pan, Z. Yi, G. Qu, and G. Shi, “Full-order sampling-based mpc for torque-level locomotion control via diffusion-style annealing,” *arXiv preprint arXiv:2409.15610*, 2024.
- [19] C. Pan, Z. Yi, G. Shi, and G. Qu, “Model-based diffusion for trajectory optimization,” *Advances in Neural Information Processing Systems*, vol. 37, pp. 57914–57943, 2024.
- [20] T. Pang and R. Tedrake, “A convex quasistatic time-stepping scheme for rigid multibody systems with contact and friction,” in *2021 IEEE International Conference on Robotics and Automation (ICRA)*. IEEE, 2021, pp. 6614–6620.
- [21] A. K. Jain, V. Mohta, S. Kim, A. Bhardwaj, J. Ren, Y. Feng, S. Choudhury, and G. Swamy, “A smooth sea never made a skilled sailor: Robust imitation via learning to search,” *arXiv preprint arXiv:2506.05294*, 2025.
- [22] M. Dalal, J. Yang, R. Mendonca, Y. Khaky, R. Salakhutdinov, and D. Pathak, “Neural mp: A generalist neural motion planner,” *arXiv preprint arXiv:2409.05864*, 2024.
- [23] J. Carvalho, A. T. Le, M. Baiert, D. Koert, and J. Peters, “Motion planning diffusion: Learning and planning of robot motions with diffusion models,” in *2023 IEEE/RSJ International Conference on Intelligent Robots and Systems (IROS)*. IEEE, 2023, pp. 1916–1923.
- [24] J. Urain, A. T. Le, A. Lambert, G. Chalvatzaki, B. Boots, and J. Peters, “Learning implicit priors for motion optimization,” in *2022 IEEE/RSJ International Conference on Intelligent Robots and Systems (IROS)*. IEEE, 2022, pp. 7672–7679.
- [25] C. Gonzalez, H. Asadi, L. Kooijman, and C. P. Lim, “Neural networks for fast optimisation in model predictive control: A review,” *arXiv preprint arXiv:2309.02668*, 2023.
- [26] J. Carius, F. Farshidian, and M. Hutter, “Mpc-net: A first principles guided policy search,” *IEEE Robotics and Automation Letters*, vol. 5, no. 2, pp. 2897–2904, 2020.
- [27] P. M. Julbe, J. Nubert, H. Hose, S. Trimpe, and K. J. Kuchenbecker, “Diffusion-based approximate mpc: Fast and consistent imitation of multi-modal action distributions,” *arXiv preprint arXiv:2504.04603*, 2025.
- [28] A. Li, Z. Ding, A. B. Dieng, and R. Beeson, “Diffusolve: Diffusion-based solver for non-convex trajectory optimization,” *arXiv preprint arXiv:2403.05571*, 2024.
- [29] T.-Y. Huang, A. Lederer, N. Hoischen, J. Brüdigam, X. Xiao, S. Sosnowski, and S. Hirche, “Toward near-globally optimal nonlinear model predictive control via diffusion models,” *arXiv preprint arXiv:2412.08278*, 2024.
- [30] A. Wächter and L. T. Biegler, “On the implementation of an interior-point filter line-search algorithm for large-scale nonlinear programming,” *Mathematical programming*, vol. 106, pp. 25–57, 2006.
- [31] J. Sacks and B. Boots, “Learning sampling distributions for model predictive control,” in *Conference on Robot Learning*. PMLR, 2023, pp. 1733–1742.
- [32] T. Power and D. Berenson, “Learning a generalizable trajectory sampling distribution for model predictive control,” *IEEE Transactions on Robotics*, 2024.
- [33] E. Todorov, T. Erez, and Y. Tassa, “Mujoco: A physics engine for model-based control,” in *2012 IEEE/RSJ international conference on intelligent robots and systems*. IEEE, 2012, pp. 5026–5033.
- [34] R. Y. Rubinfeld and D. P. Kroese, *The cross-entropy method: a unified approach to combinatorial optimization, Monte-Carlo simulation and machine learning*. Springer Science & Business Media, 2004.
- [35] Y. Lipman, R. T. Chen, H. Ben-Hamu, M. Nickel, and M. Le, “Flow matching for generative modeling,” *arXiv preprint arXiv:2210.02747*, 2022.
- [36] J. Ho, A. Jain, and P. Abbeel, “Denoising diffusion probabilistic models,” *Advances in neural information processing systems*, vol. 33, pp. 6840–6851, 2020.
- [37] A. Tong, K. Fatras, N. Malkin, G. Hugué, Y. Zhang, J. Rector-Brooks, G. Wolf, and Y. Bengio, “Improving and generalizing flow-based generative models with minibatch optimal transport,” *arXiv preprint arXiv:2302.00482*, 2023.
- [38] X. Zhu, Y. Chen, L. Sun, F. Niroui, S. Le Cleac’h, J. Wang, and K. Fang, “Versatile loco-manipulation through flexible interlimb coordination,” *arXiv preprint arXiv:2506.07876*, 2025.
- [39] A. Li, S. L. Cleac’h, B. Hung, A. D. Ames, J. Wang, and P. Culbertson, “Judo: A user-friendly open-source package for sampling-based model predictive control,” in *Proceedings of the Workshop on Fast Motion Planning and Control in the Era of Parallelism at Robotics: Science and Systems (RSS)*, 2025. [Online]. Available: <https://github.com/bdaiinstitute/judo>
- [40] T. Anthony, Z. Tian, and D. Barber, “Thinking fast and slow with deep learning and tree search,” *Advances in neural information processing systems*, vol. 30, 2017.

APPENDIX

A. Implementation Details

We describe the implementation of our generative model and sampling-based MPC algorithm, used for both offline data collection and online control. Code for data collection, model training and the bootstrapped SPC controller will be released upon acceptance.

Data Collection: We collect training data using a sampling-based MPC controller in simulation for a maximum of 2500 time steps per episodes in both tasks, which generates open-loop control sequences. For Push-T, trajectories are cubic splines with 4 control points; for Spot, they consist of 4 linearly interpolated waypoints. All data is represented in the world frame, not relative to the robot. Although we tested robot-centric representations, they did not yield performance improvements. We collected 67,667 Push-T sequences from 1,000 successful episodes and 211,832 Spot sequences from 1,700 episodes. For evaluation, we use fixed sets of randomly sampled initial states for each task, shared across all methods and runs to ensure consistency.

Training Details: We train a conditional flow-matching model with simple MLPs, using a batch size of 40,000 and the Adam optimizer (learning rate 0.0001, cosine annealing schedule, 500 warmup steps) over 1,000 epochs. The model predicts 4 control points conditioned on the current robot and object state and the previous replanning state (history length = 1). Orientations are represented using sine-cosine encodings of yaw angles. Although Spot expects velocity commands, we predict absolute positions and convert them to velocities via finite differences during online control.

Cost Functions: Both tasks use a weighted sum of cost terms computed over the full-resolution control sequence (0.01s for Push-T, 0.02s for Spot). The cost components are:

- 1) *Robot-Object Proximity:* L2 distance between the robot and object. For Spot, we penalize both torso and end-effector distances.
- 2) *Velocity Penalty:* L2 norm of robot joint velocities.

- 3) *Goal Reaching*: L2 distance and angle difference between object and goal, plus a progress term penalizing lack of advancement over time.
- 4) *Joint Limits (Spot)*: Penalty for exceeding arm joint limits (leg joints are handled by the low-level policy).
- 5) *Fall Penalty (Spot)*: Large penalty if the torso height drops below a threshold, preventing falls.
- 6) *Object Tipping (Spot)*: Large penalty if the chair's z-axis deviates from vertical, discouraging it from tipping over.

Weights were tuned empirically and will be provided in the released code.